Nano Trends 10 (2025) 100103

Contents lists available at ScienceDirect

Nano Trends

journal homepage: www.elsevier.com/locate/nantre

Elucidating the role of nano boron and zinc oxide-coated silane-treated cellulose nanocrystals (CNCs) on the mechanical, thermal, and flammability characteristics of high-density polyethylene (HDPE)

Amirmohammad Raeisi [a], Ismat Ara [a], Greg Holt [b], Nicole Stark [c], Dilpreet S. Bajwa [a,*]

[a] Department of Mechanical & Industrial Engineering, Montana State University, Bozeman, MT 59715, USA
[b] Cotton Production and Processing Research Unit, USDA-ARS, Lubbock, TX, USA
[c] USDA Forest Products Laboratory, Madison, WI, USA

ARTICLE INFO

Keywords:
Cellulose nanocrystals
High-density polyethylene
Mechanical properties
Nano boron oxide
Nano zinc oxide
Silane-functionalized CNCs

ABSTRACT

The fire risk of synthetic polymers has emerged as a growing safety issue. High-density polyethylene (HDPE) is one of the most used polymers in different applications. However, HDPE has some drawbacks, such as low thermal and mechanical properties. To address this challenge, silane-functionalized cellulose nanocrystals (CNCs), nano boron oxide (B_2O_3) and nano zinc oxide (ZnO) were incorporated into the HDPE matrix in different percentages (3 %, and 5 %) and weight ratios (1:1, and 1:2). The CNCs were surface modified through silanization process to enhance dispersion and interfacial bonding, while metal oxides were introduced to improve thermal stability and flame retardancy. The composites were characterized using scanning electron microscopy (SEM), dynamic mechanical analyzer (DMA), differential scanning calorimetry (DSC), Fourier transform infrared spectroscopy (FTIR), thermogravimetric analyzer (TGA), horizontal burn test, and microcalorimetry tests. The results indicated that adding CNCs-ZnO resulted in a 64 % increase in mechanical properties, a 28 % decrease in weight loss, and a reduced flame spread rate of the composites. The CNCs- B_2O_3 composites showed a lower flame spread rate and a 52 % improvement in mechanical properties. Overall, adding nano metallic fillers, such as nano ZnO and B_2O_3, significantly enhanced HDPE composites' thermal stability, mechanical properties, and fire resistance. These improvements highlight the potential of nano metal oxides and CNC as functional fillers where mechanical strength and fire safety are essential.

1. Introduction

The development of polymer composites has been an area of intense research over the past few decades. The utilization of bio-based polymers and composites helps mitigate the negative impact and environmental damage of fossil fuel-derived polymers. Nevertheless, biobased polymers often have poor mechanical properties, which can be resolved by the incorporation of fibers and biofilters into the polymer matrix [1,2]. Another issue is that synthetic polymeric materials suffer from intrinsic high flammability, which limits their applications [1,3]. HDPE is one of the most widely utilized polymers in various applications, including packaging, automotive, and construction, owing to its lightweight nature, chemical resistance, and ease of processing [4]. However, HDPE suffers from low mechanical and thermal properties. To address these drawbacks, reinforcement materials are specialty chemicals are added to HDPE to improve its strength, fire resistance, and thermal characteristics.

Fire resistance of the polymers is related to their ability to handle high temperatures and resist combustion. Combustion of a polymer includes four stages (1) pyrolysis when exposed to heat, (2) flammable gas release, (3) combustion due to mixing of oxygen with released gases, and (4) heat release by flame propagation. To improve the fire-retardancy of polymeric materials, this cycle should be stopped [5]. Fire-retardant nanocomposite materials have become a significant subset of the nanocomposite field. The two modes that a fire retardant can act in to stop this cycle are by producing a non-flammable gas in the gas phase and the other by creating an insulating char layer in the condensed phase [5,6]. An insulating char layer acts as a barrier, reduces heat transfer, limits oxygen diffusion, and slows down the release of volatile combustibles, and results in improved fire retardancy.

* Corresponding author.
E-mail address: dilpreet.bajwa@montana.edu (D.S. Bajwa).

https://doi.org/10.1016/j.nwnano.2025.100103
Received 31 December 2024; Received in revised form 27 February 2025; Accepted 16 March 2025
Available online 17 March 2025

The primary compounds that enhance fire retardancy are minerals, silicon-based, phosphorus-based, halogen-based, and nanometric compounds [7]. Despite the effective role of halogen-based fire retardants in improving fire resistance in polymers, their utilization has been banned because of their production of harmful gases when burned and their negative impact on the environment and human health [7,8]. Some non-toxic inorganic mineral fillers, such as montmorillonite, magnesium hydroxide, and calcium carbonate, are considered safe fire retardants. However, their flame-retardant effectiveness is low, meaning that significant quantities are needed to reach the desired flame-retardant performance [9,10]. Phosphorus-based flame retardants have gained significant attention in the field of fire safety for polymeric materials due to their high flame retardancy efficiency and versatile mechanisms of action. These flame retardants can improve fire resistance by working in both gas and condensed phases to enhance fire resistance. In the gas phase, they can capture free radicals, while in the condensed phase, they promote carbonization, which inhibits heat exchange and the release of pyrolysis volatiles [10,11]. A study explored the synergistic impact of ammonium polyphosphate (APP) combined with three different phosphorus-based flame retardants, such as pentaerythritol phosphate (PEAP), aluminum diethylphosphinate (ADP), and phenoxycyclophosphazene (PCP) on the fire resistance and mechanical properties of rigid polyurethane foam (RPUF) composites [12]. The findings revealed that these flame retardants significantly enhanced the fire resistance of RPUF composites through mechanisms occurring in both the condensed and gas phases. This improvement was attributed to the formation of char during thermal degradation, which created an insulating barrier over the polymer. However, concerns have been raised regarding phosphorus-based compounds due to their ability to produce significant amounts of smoke, their inherent toxicity, and the associated risks they pose to human health and the environment [13,14].

Cellulosic and lignocellulosic materials are widely employed to improve mechanical properties and retain the biodegradability of biopolymers. Cellulose is a naturally derived, biodegradable polymer that forms the structural framework of plant cell walls. In addition to plants, it is also produced by algae, specific bacteria, such as *Acetobacter*, and certain marine organisms, making it the most widely occurring polymer on earth [15]. Due to its abundance, cellulose is essential in both biological systems and numerous industrial applications [15]. Cellulose nanocrystals (CNCs), needle-like highly crystalline cellulosic materials, are produced using acid hydrolysis [1,5]. CNCs are widely employed in strengthening polymers due to their superior mechanical properties, good thermal stability, high aspect ratio of 10–70, high surface area of 150 m^2/g, and biodegradability, making them suitable for different applications such as packaging, biomedical materials, and sustainable composites [16]. Upon degradation, cellulose forms charred structures. At low temperatures and low heating rates, cellulose experiences dehydration reactions, which leads to its rearrangement and the formation of char [17]. In addition, it has been reported that even low concentrations of inorganic salts have a catalytic effect when combined with cellulose, improving its thermal stability and enhancing char formation [18,19].

However, CNCs have a high tendency to form agglomerates due to the presence of hydroxyl groups on their surface, which makes it difficult to use them for different applications. The abundant hydrogen bonds of cellulose draw the cellulose nanocrystals together and result in the forming of bundles or aggregates [16]. One advantage of using CNCs is that the presence of hydroxyl groups facilitates modifications through various functionalization reactions, including etherification, esterification, oxidation, silanization, and crosslinking reactions [15,20]. Several chemical surface modification methods, such as silanization, have been reported to be effective for altering the hydrophilic nature of CNCs and improving their dispersion. Additionally, silanization enhances CNCs' thermal stability by covering the sulfate ester groups formed on their surface during sulfuric acid hydrolysis and also improves the mechanical performance of the composites [21]. Previous research has shown that incorporating silane-treated CNCs into a polyethylene oxide (PEO) matrix enhanced the mechanical and thermal properties of nanocomposite thin films by improving filler dispersion and increasing char formation [21].

Recent studies have highlighted the potential of inorganic materials, such as zinc oxide (ZnO) and boron-based compounds, in enhancing fire resistance. The use of zinc oxide (ZnO) particles has been found to enhance fire retardance and UV protection in pine wood [19]. The optimization of the synergistic effect of silica and ZnO has demonstrated enhanced fire resistance properties of cotton fabric while preserving its mechanical and comfort properties [22]. In addition, ZnO nanoparticles and phytic acid (PA) have shown significant promise due to their synergistic fire-resistant properties [23]. ZnO nanoparticles act as a thermal barrier by preventing heat propagation, while PA facilitates char formation, reducing oxygen supply at the combustion site. These materials have been particularly effective in enhancing the flame resistance of polyurethane (PU) coatings, which are widely used in automotive finishes, wood furniture, flooring, electronics, and marine applications [23]. Another study on the combustion properties of cotton treated with ZnO particles revealed that the ZnO particles created a consistent protective layer on the cotton's surface [24]. This resulted in a reduced peak heat release rate (PkHRR), fire growth rate (FIGRA), and maximum average rate of heat emission (MARHE) compared to untreated cotton.

Boron-based compounds also are quickly emerging as a new category of safe fire-retardant materials. It is observed that boron compounds, irrespective of their type, lower the maximum decomposition temperature and enhance the char formation [25]. The combination of boron compounds (zinc borate (ZB), boron phosphate (BPO_4), and boron oxide (B_2O_3)) combined with a phosphaphenanthrene compound (TAD) in epoxy resin (EP) thermosets has shown a highly effective synergistic flame-retardant mechanism, balancing gas-phase and condensed-phase effects [26]. Among the formulations B_2O_3/TAD had the best flame-retardant effect. B_2O_3 strengthened the condensed-phase flame--retardant effect, interacting with the epoxy matrix to enhance char formation, while TAD worked in the gas-phase by releasing PO and phenol free radicals, which suppressed flames and reduced heat. The incorporation of boric acid (BA) and boron oxide (B_2O_3) into polyamide-6 (PA) and glass fiber-reinforced polyamide-6 (PA/GF) has been shown to significantly enhance flame retardancy [27]. The use of boron oxide and boric acid results in the formation of a glass-like protective layer, which limits oxygen flow to the polymer surface, causing polymer dehydration and the formation of char. Zinc oxide and boron oxide offer several advantages in comparison with traditional fire retardants, such as their affordability, high surface reactivity, and have a lower environmental impact because of their low toxicity and reduced smoke production [6].

In this paper, we utilized a hybrid filler system consisting of silane-treated cellulose nanocrystals (CNCs) and nano-sized inorganic metal oxides such as zinc oxide and boron oxide for polyethylene-based composites. The underlying hypothesis is that incorporating this hybrid nanometric system into the high-density polyethylene (HDPE) matrix would improve fire resistance properties of HDPE by creating as surface barrier. The goal of this study was to evaluate a fire retardant for HDPE that is both safe, effective, and environmentally friendly. This research aligns with sustainability goals by utilizing bio-derived CNCs and eco-friendly metal oxides, reducing reliance on petroleum-based additives and hazardous flame retardants. By transforming cellulose into afunctional reinforcement material, this study contributes to the advancement of sustainable polymer composites, offering a greener alternative for industries requiring both durability and fire safety.

2. Materials and methods

2.1. Materials

High-density polyethylene (HDPE) powder, having a melting point

of 126 °C and a melt index of 3.5 g/10 min, was sourced from Nova Chemical and used as matrix material. Cellulose nanocrystals (CNCs), measuring 80–100 nm in length and 10–15 nm in width, with the resulting aspect ratios ranging from 5 to 10, were supplied by the USDA Forest Products Laboratory (Madison, WI, USA). These CNCs were obtained through acid hydrolysis of softwood pulp and further treated via a hydrothermal desulphation process. (3-Aminopropyl) triethoxysilane (APES), with a purity of 98 % and a molecular weight of 221.37 g/mol, was supplied by Sigma Aldrich. Zinc acetate dihydrate and sodium hydroxide, also from Sigma Aldrich, were used to synthesize zinc oxide (ZnO). Methanol, acquired from the chemistry store at Montana State University, served as the solvent in the ZnO production process. Boron oxide powder and oleic acid, both from Sigma Aldrich, were utilized to prepare nano boron oxide. Deionized water, obtained from Millipore, USA, served as solvent throughout the process.

2.2. CNCs' surface modification by silanization

The procedure of surface modification of CNCs was performed following the method outlined in the literature [21,28]. Initially, one gram of CNCs was dissolved in deionized (DI) water while continuously stirring at room temperature. Next, APES was introduced to the solution in a 1:1 wt ratio with CNCs, and the solution was stirred for 30 min. Finally, the solution was heated to 90 °C to initiate the silanization of the surface hydroxyl groups on the CNCs.

2.3. B_2O_3 coated silane-treated CNCs synthesis

The nano B_2O_3 was synthesized following the previously reported method [6]. Initially, 0.2 g of boron oxide (B_2O_3) granules were ground to a coarse powder using an agate mortar and pestle. The powder was placed into a 100 mL centrifuge tube, and 10 mL of oleic acid was added. The mixture then was sonicated at an amplitude of 50 % for 3 h while maintained in an ice bath. Afterward, to remove the supernatant oleic acid, the mixture was centrifuged at 9000 rpm for 15 min. The solid residue was washed with 10 mL of anhydrous hexane and then vacuum dried to produce a white fluffy powder. This B_2O_3 powder was then mixed with aqueous dispersions of silane-treated CNCs at weight ratios of 1:1 and 1:2. The final blends were sonicated and freeze-dried for use in polymer nanocomposites.

2.4. ZnO coated silane-treated CNCs synthesis

The nano ZnO were synthesized following a procedure described in an earlier study [29]. First, 0.08 mol of sodium hydroxide was combined with 100 mL of methanol and heated to 50 °C while stirring vigorously for 1 hour to form precursor solution A. At the same time, precursor B was made by dissolving 0.04 mol of Zinc acetate dehydrate in 100 mL of methanol at 50 °C, with vigorous stirring for 30 min. Solutions A and B were then mixed dropwise at 50 °C under constant stirring to produce a ZnO nano-solution. The mixture was stirred for 2 h, then allowed to cool at room temperature to yield a transparent ZnO solution. This solution was freeze-dried and mixed with aqueous silane-treated CNCs dispersion at weight ratios of 1:1 and 1:2. The resulting mixture was sonicated and freeze-dried to use in nanocomposites.

2.5. HDPE composites preparation

The composite samples were fabricated using a dual screw extruder (Thermo Fisher Scientific HAAKE Minilab II), followed by injection molding. The extrusion was performed at 150 °C for 5 min and 100 rpm with filler weight percentages of 3 % and 5 %. Following extrusion, the composites were injected into a Thermo Fisher Scientific Minijet Pro injection molder. The samples were molded into a flexural sample mold. The samples dimensions were 60 mm × 10 mm × 1 mm. The injection molding gun temperature was 150 °C, and the mold was maintained at 95 °C. The samples were injection molded at a pressure of 650 bar for 10 s, followed by a post-pressure of 400 bar for 20 s. The extrusion and injection molding processing parameters were chosen based on a previous study to prevent degradation of the fillers and polymer matrix [6]. The samples compositions are provided in Table 1.

2.6. Characterization

2.6.1. Scanning electron microscopy (SEM)

The samples were fractured under a liquid nitrogen environment to ensure clean breaks, and the resulting cross-sectional morphology was analyzed using scanning electron microscopy (SEM). For optimal conductivity, the samples were coated with a thin iridium layer. Cross-sectional images were taken at varying magnifications using a field emission scanning electron microscope (Supra 55VP, Zeiss, Thornwood, NY, USA), which was set at an accelerating voltage of 2.0 kV. These analyses were conducted at the Image and Chemical Analysis Laboratory (ICAL) at Montana State University.

2.6.2. Fourier transform infrared spectroscopy (FTIR)

To analyze the composite samples, Fourier-transform infrared (FTIR) spectroscopy was conducted using a Thermo-Scientific Nicolet i550 FTIR/ATR spectrometer (ThermoFisher Scientific, Madison, WI). The experiment employed an attenuated total reflection (ATR) mode utilizing an ID7/ITX AR coated diamond crystal. Each spectrum was collected by conducting 64 scans at a resolution of 4 cm^{-1}, across a wavenumber ranging from 500 to 4000 cm^{-1}.

2.6.3. Dynamic mechanical analysis (DMA)

The dynamic storage and loss modulus of the composite samples were measured using a TA Instruments Dynamic mechanical analyzer (Q800) (TA Instruments, New Castle, DE, USA). The experiments were conducted in 3-point bending mode in a temperature range of 30 to 110 °C, an amplitude of 15 μm, a force track of 125 %, and a constant frequency of 1 Hz. For each formulation, a minimum of 3 replicates were tested and average values were reported.

2.6.4. Differential scanning calorimetry (DSC)

A TA Instrument Differential scanning calorimetry (DSC), model (Q2500, New Castle, USA), was used to measure fusion enthalpy and melting peak of the composite samples. Approximately 6–7 mg of each formulation was tested in a nitrogen atmosphere. The samples were scanned across a temperature range from 30 to 250 °C at a heating rate of 10 °C/min. The crystallinity (X_c) was calculated using the following equation:

Table 1
Compositions of composite samples.

Formulation	Matrix (HDPE) (wt %)	CNCs (Ratio)	ZnO (Ratio)	B_2O_3 (Ratio)
Pure HDPE	100	–	–	–
H-3CS	97	1	–	–
H-5CS	95	1	–	
H-3(Z1CS1)	97	1	1	–
H-5(Z1CS1)	95	1	1	–
H-3(Z2CS1)	97	1	2	–
H-5(Z2CS1)	95	1	2	–
H-3(B1CS1)	97	1	–	1
H-5(B1CS1)	95	1	–	1
H-3(B2CS1)	97	1	–	2
H-5(B2CS1)	95	1	–	2

* Each formulation code indicates the filler percentage and weight ratios. For instance, H-3CS shows that the composite consists of 97 wt.% HDPE and 3 wt.% silane-treated CNCs. Sample H-5(B2CS1) shows 95 wt.% HDPE and 5 wt.% filler, with the filler composed of a ratio of 2 parts boron oxide to 1 part silane-treated CNCs.

$$X_c(\%) = \frac{\Delta H_m}{\Delta H_m^0} \times 100 \times (1 - x) \quad (2)$$

Where ΔH_m is the melting enthalpy, ΔH_m^0 represents the melting enthalpy of 100 % crystalline HDPE (293 J g^{-1}), and x denotes weight fraction of filler (ZnO-coated CNCs or B_2O_3-coated CNCs).

2.6.5. Thermogravimetric analysis

Thermogravimetric analysis was performed using a Linseis Thermowaage L81 instrument at Montana State University (LINSEIS, Robbinsville Township, New Jersey, USA). The tests were performed within a temperature range of 30 °C to 600 °C, at a heating rate of 10 °C per minute, and under an argon atmosphere.

2.6.6. Horizontal burn test

The composite samples, each with dimensions of 60 mm x 10 mm x 1 mm and a rectangular shape, were tested in accordance with ASTM D635–14 standard. During the test, the samples were positioned horizontally on the mount with their longitudinal axis aligned. To ignite the samples, a butane lighter was utilized, with the flame directed at a 45° angle towards the free end of the sample. Three samples of each formulation were tested, and the average values were reported.

2.6.7. Microcalorimetry test

A microscale combustion calorimeter (MCC, Fire Testing Technology Ltd., Gosport, UK) was used to perform pyrolysis-combustion flow calorimetric measurements by Infinita Lab Inc. (California, USA) following ASTM D7309 standard. From these measurements, the flammability and combustion of samples were investigated. About 3 mg of each sample were individually heated to 900 °C with a heating rate of 1 °C/s. A stream of nitrogen (80 cm^3 /min) and oxygen (20 cm^3 /min) were mixed with volatile degradation products before entering the combustion chamber.

2.6.8. Statistical analysis

The statistical analysis of dynamic and mechanical properties as well as burn tests of the composite samples were performed using Minitab software version 22 (Minitab Inc., State College, PA, USA). ANOVA and Fisher mean comparison tests were conducted to identify significant difference between composite formulations and to calculate mean and standard deviations with a significance level of $\alpha = 0.05$.

3. Results and discussion

3.1. Scanning electron microscopy (SEM)

The cryo-fractured surface of the composites containing only silane-treated CNCs and composites containing inorganic metal oxides were investigated through SEM to evaluate the influence of fillers on HDPE composite microstructure. Fig. 1 demonstrates the dispersion quality of fillers in the HDPE matrix. SEM micrographs showed distinct morphological features across different composite formulations. The silane-treated CNCs composite with lower CNCs concentrations (H-3CS) displayed a relatively ductile fracture surface with lower filler aggregation. As the filler concentration increased to 5 wt% (H-5CS), more pronounced filler clustering and surface irregularities became evident. Generally, higher CNCs concentrations result in a greater number of aggregates [30]. Similarly, Composites modified with zinc oxide (H-3(Z2CS1), H-5(Z2CS1), boron oxide (H-3(B2CS1), and H-5(B2CS1)) showed progressively rougher surface textures with increasing filler concentrations. Typically, the mechanical properties of composites are linked to their morphology. For instance, a rough and irregular fractured surface can be indicative of greater material toughness [31]. The rougher fractured surface is tougher. This means higher energy and work is needed to fracture these samples, which is evidenced through DMA test results. The observations are consistent with findings from other studies, which indicate that a rougher fractured surface observed in SEM lead to higher mechanical properties in poly (lactic acid)-CNCs composites [32].

3.2. Fourier transform infrared spectroscopy (FTIR)

FTIR testing was performed to analyze the chemical structures of the materials after undergoing melt extrusion. Fig. 2 depicts the FTIR spectra for pure HDPE and all composites containing CNCs-zinc oxide and CNCs-boron oxide with different percentages and weight ratios. The bands around 2920 cm^{-1} and 2850 cm^{-1} correspond to asymmetric and symmetric stretching of C—H bands, respectively. The bands observed around 1470 cm^{-1} and 720 cm^{-1} signify CH_3 bending vibration and CH_2 rocking vibration, respectively [33]. For all composite samples containing silane-treated CNCs and metal oxides, there is an increase in the intensity of absorbance at these peaks due to the overlap between the cellulose -C-H stretching band and the HDPE stretching band. Some formulations with higher metal oxide percentages and weight ratios

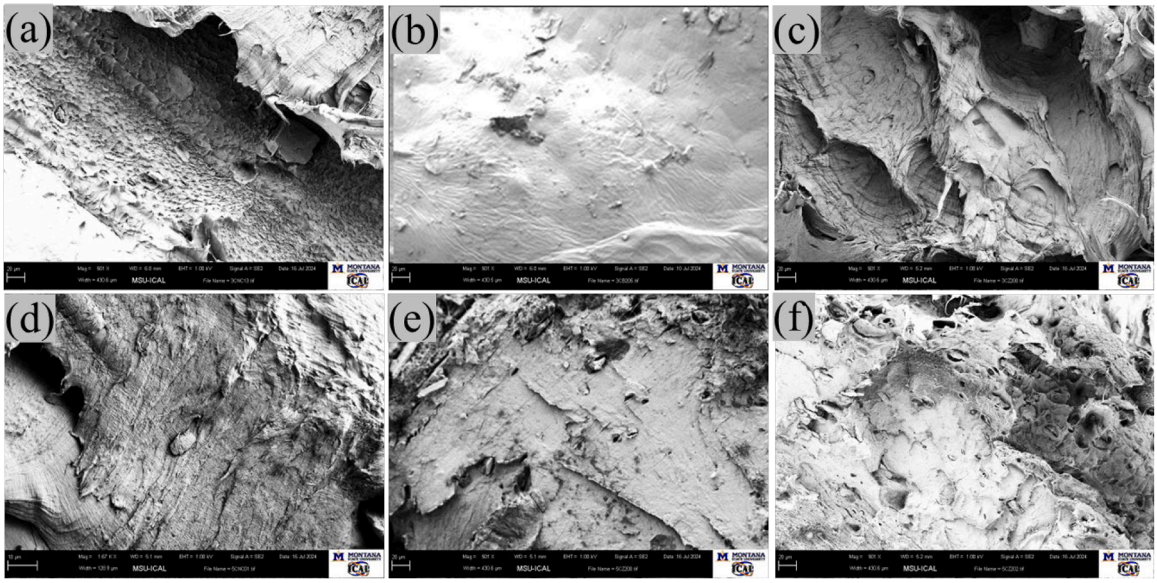

Fig. 1. SEM micrograph of fractured surface of the composites (a) H-3CS, (b) H-3(B2CS1), (c) H-3(Z2CS1), (d)H-5CS, (e) H-5(B2CS1), (f) H-5(Z2CS1).

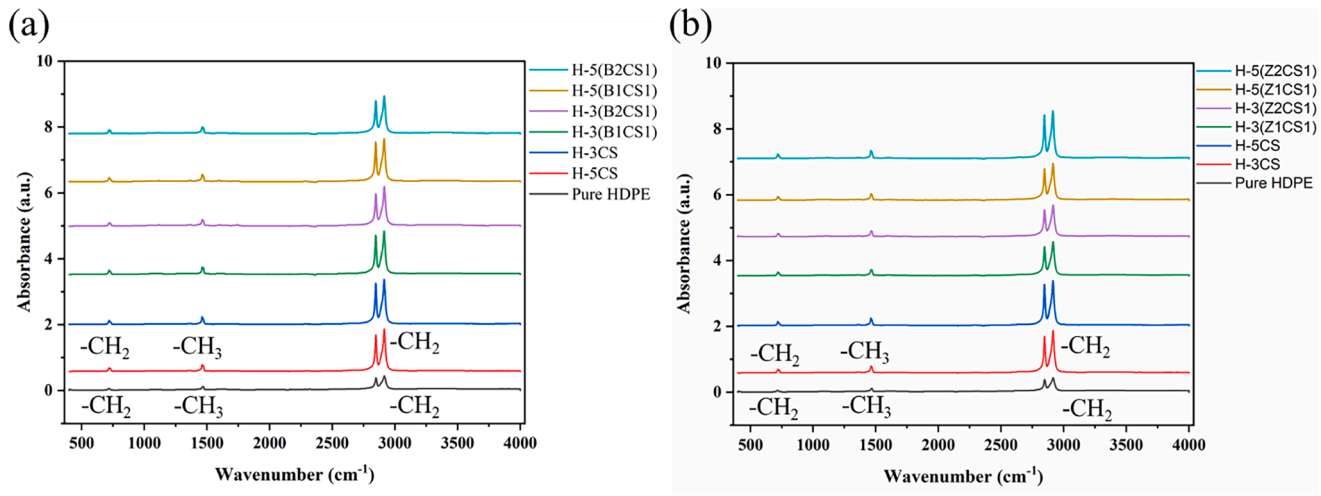

Fig. 2. FTIR spectra of pure HDPE and HDPE composites of silane-functionalized CNCs with(a)B_2O_3 and (b) ZnO.

show lower intensities, likely due to the filler agglomeration [34]. Overall, the results show the successful incorporation of CNCs into the system.

3.3. Dynamic mechanical analysis (DMA)

Viscoelastic behavior and dynamic mechanical properties as a function of temperature for all composites were assessed using a dynamic mechanical analyzer (DMA). Storage and loss modulus of the composites at different temperatures are provided in Figs. 3 and 4, and Tables 2 and 3. The storage modulus of the pure HDPE is shown to be 747.47 MPa. It was observed that the filler concentration had a significant effect on the composites' dynamic mechanical properties. The incorporation of silane-treated CNCs increased the storage modulus values significantly. Additionally, higher filler contents resulted in higher storage moduli of the composites. This is attributed to the increased reinforcement effect provided by fillers and the reduction in polymer chain mobility, which consequently raises the flow resistance of HDPE [29]. The same trend was observed for loss modulus values, which is indicative of viscous or non-recoverable components of the composites. Higher filler concentration also led to higher loss modulus, which demonstrates that while higher filler concentration contributes to higher stiffness, it also increases energy dissipation and damping characteristics of the composites [35]. Moreover, the incorporation of B_2O_3-coated silane-functionalized CNCs also provided enhancements in both storage and loss modulus compared to pure HDPE samples. Among the formulations, H-5(B1CS1), containing 5 wt.% filler with a 1:1 ratio of boron oxide to silane-treated CNCs, exhibited the highest improvement in storage and loss modulus values. This enhanced performance in H-5 (B1CS1) samples is attributed to the synergistic effects of combining B_2O_3 with silane-functionalized CNCs which improved matrix-filler interactions and restricted polymer chain mobility, resulting in superior mechanical properties [36].

Fig. 4 and Table 3 provide the DMA test results for composite samples with silane-treated CNCs/ZnO. The same trend in the storage and loss modulus of the composite samples was observed. The addition of nano-zinc oxide further significantly enhanced the value of storage modulus. Higher filler concentration resulted in higher storage modulus while higher ratio of ZnO did not show any significant impact on the values.

Overall, the storage modulus of composites with ZnO-coated silane-treated CNCs increased by 64 %, and the modulus of composites with B_2O_3-coated silane-treated CNCs increased by 52 % compared to pure HDPE.

3.4. Differential scanning calorimetry (DSC)

The crystallization and melting behavior of the composites was

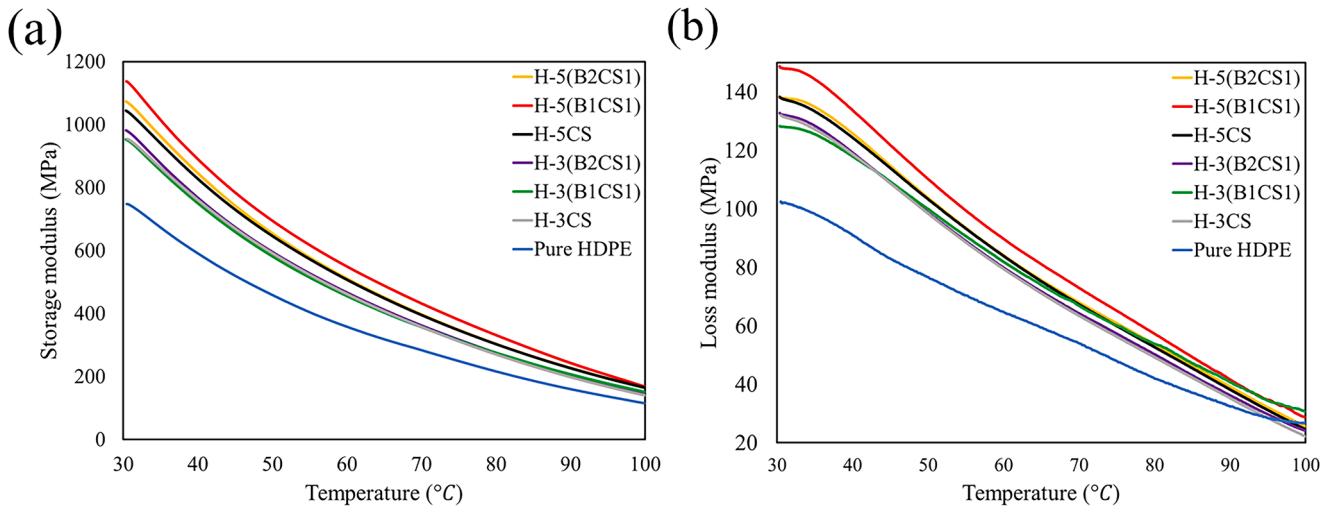

Fig. 3. Representative curves of (a) storage modulus and (b) loss modulus as a function of temperature for B_2O_3-coated CNCs samples.

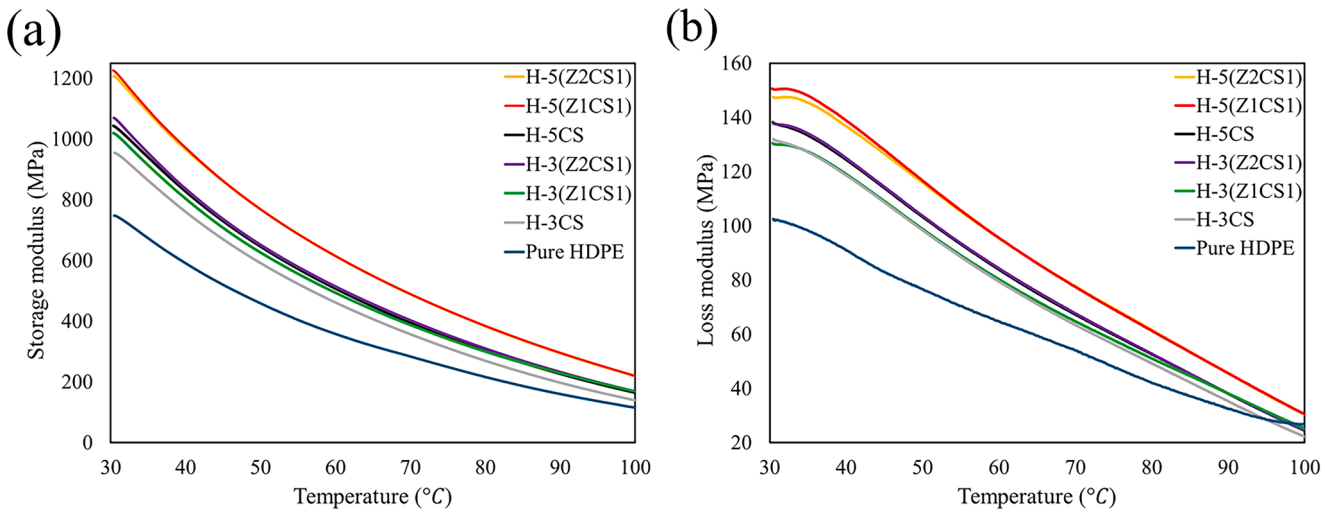

Fig. 4. Representative curves of (a) storage modulus and (b) loss modulus as a function of temperature for ZnO-coated CNCs samples.

Table 2
Storage and loss modulus values of composites containing CNCs-Boron oxide at different temperatures.

Formulation	Storage Modulus (MPa)		Loss Modulus (MPa)	
	30 °C	70 °C	30 °C	70 °C
Pure HDPE	747.47±37.2^{a}	282.85±15.1^{a}	102.44±4.1^{a}	53.8 ± 1.1^{a}
H-3CS	946.5 ± 49.6^{b}	353.6 ± 19.1^{b}	132.1 ± 3.13^{b}	63.3 ± 2.0^{b}
H-5CS	1043.9 ± 30.4^{c,d}	395.0 ± 23.2^{c}	138.2 ± 3.5^{c}	67.2 ± 2.8^{b}
H-3(B1CS1)	952.4 ± 54.4^{b}	355.9 ± 28.5^{b}	128.2 ± 2.87^{b}	66.6 ± 4.3^{b}
H-5(B1CS1)	1136.8 ± 25.7^{e}	431.3 ± 13.5^{d}	148.7 ± 3.70^{d}	72.8 ± 1.9^{c}
H-3(B2CS1)	982.3 ± 20.2^{b,c}	361.2 ± 9.4^{b}	132.8 ± 0.8^{b}	64.1 ± 0.2^{b}
H-5(B2CS1)	1073.2 ± 43.2^{d,e}	397.3 ± 17.6^{c,d}	138.3 ± 3.0^{c}	67.8 ± 2.9^{b}

*Values (mean ± SD) in each column with different letters are significantly different from one another, according to Fisher's least significant difference test at α = 0.05.

Table 3
Storage and loss modulus values of composites containing CNCs-Zinc oxide at different temperatures.

Formulation	Storage Modulus (MPa)		Loss Modulus (MPa)	
	30 °C	70 °C	30 °C	70 °C
Pure HDPE	747.47±37.2^{a}	282.85±15.1^{a}	102.44±4.1^{a}	53.8 ± 1.1^{a}
H-3CS	946.5 ± 49.6^{b}	353.6 ± 19.1^{b}	132.1 ± 3.13^{b,c}	63.3 ± 2.0^{b}
H-5CS	1043.9 ± 30.4^{c}	395.0 ± 23.2^{c}	138.2 ± 3.5^{c}	67.2 ± 2.8^{b}
H-3(Z1CS1)	1020.0 ± 54.9^{c}	387.1 ± 30.7^{b,c}	130.5 ± 8.38^{b}	64.6 ± 4.6^{b}
H-5(Z1CS1)	1226.3 ± 14.4^{d}	488.7 ± 2.1^{d}	150.6 ± 2.78^{d}	77.3 ± 1.3^{c}
H-3(Z2CS1)	1069.4 ± 32.8^{c}	403.6 ± 20.1^{c}	138.0 ± 2.91^{b,c}	67.7 ± 1.94^{b}
H-5(Z2CS1)	1212.62±6.7^{d}	481.51±5.46^{d}	151.16±3.3^{d}	76.9 ± 0.4^{c}

* Values (mean ± SD) in each column with different letters are significantly different from one another, according to Fisher's least significant difference test at α = 0.05.

studied using DSC. Figs. 5a and 5b illustrate the DSC thermogram of the HDPE-based composites, with the corresponding thermal parameters for all samples listed in Tables 4 and 5. The glass transition temperature for Pure HDPE and its composites was not detected as it's lower than 30 °C. As shown in the DSC graphs, all the samples showed almost identical crystallization temperatures, which indicates the presence of a single homogenous phase through the heating process [32]. This suggests that the incorporating fillers did not significantly change the thermal transition temperature of the polymer matrix. However, the crystallinity of the composites with silane-treated CNCs decreased compared to pure HDPE, and higher filler concentrations resulted in even lower crystallinity values. The reason for this observation is the confinement effect of the fillers. Introducing filler restricts the chain mobility of the polymer. This restriction hinders the ability of the polymer chains to arrange into well-ordered crystalline structures, leading to lower crystallinity values [21,37]. Additionally, the higher loading ratio of boron oxide resulted in slightly further reductions in crystallinity. This reduction can be due to the presence of oleic acid in the boron oxide structure. The bulky and large structure of oleic acid, along with the aggregation of CNCs, hindered the formation of stable crystals and led to a further reduction in crystallinity values [6]. Oleic acid was incorporated into the boron oxide structure to prevent moisture absorption.

A similar trend was observed for the composite with ZnO. Higher concentrations of the ZnO resulted in lower crystallinity values. The reduction in crystallinity (X_c) observed in all composites compared to neat HDPE can be explained by a decrease in the aspect ratios of the fillers during the freeze-drying process, which caused agglomeration, as noted in previous studies [6,38].

3.5. *Thermogravimetric analysis*

The thermal stability of the composites was investigated using a thermogravimetric to assess the impact of B_2O_3 and ZnO. The findings are provided in Table 6 and Table 7. The thermal stability of samples was evaluated by comparing the T_{onset}, T_{50}, and T_{endset} values. T_{onset} indicates the initial temperature at which the composites begin to break down and degrade, T_{50} represents the temperature at which 50 % of the weight is lost, and T_{endset} is the temperature at which degradation is complete. The composite samples with only silane-treated CNCs (H-3CS and H-5CS) exhibited an increase in thermal stability, as shown by a higher T_{onset}. Initial decomposition temperature, T_{50} and T_{endset} for these samples increased because of the char formation. The addition of B_2O_3 and its higher ratio did not show any effect on the initial decomposition temperature of the composites. The reason behind this observation can

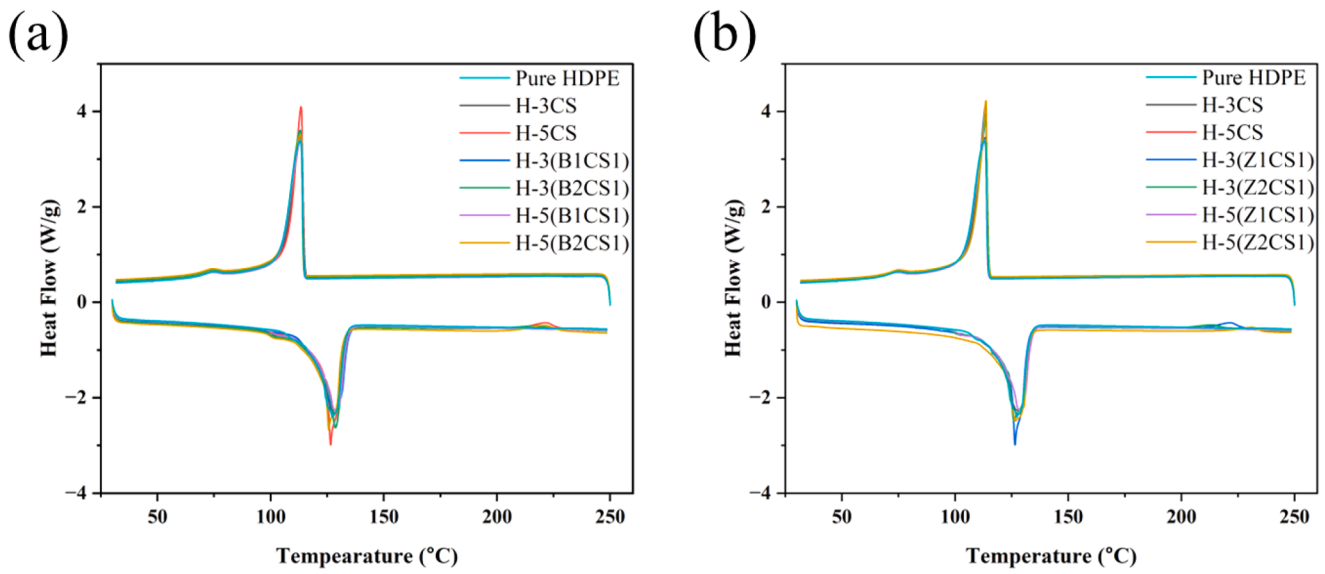

Fig. 5. DSC thermograms of (a) composites with B_2O_3-coated CNCs and (b) composites with ZnO-coated CNCs.

Table 4
Crystallization patterns of each composition (B_2O_3-coated silane-treated CNCs).

Formulation	T_c (°C)	T_m (°C)	(X_c) (%)
Pure HDPE	114.58	127.82	56.52
H-3CS	114.90	127.3	51.86
H-5CS	114.35	126.4	46.84
H-3(B1CS1)	114.23	128.27	51.75
H-3(B2CS1)	114.30	128.41	50.84
H-5(B1CS1)	114.22	127.71	45.56
H-5(B2CS1)	114.15	125.72	44.71

Table 5
Crystallization patterns of each composition (ZnO-coated Silane-treated CNCs).

Formulation	T_c (°C)	T_m (°C)	(X_c) (%)
Pure HDPE	114.58	127.82	56.52
H-3CS	114.90	127.3	51.86
H-5CS	114.35	126.4	46.84
H-3(Z1CS1)	114.84	126.04	49.50
H-3(Z2CS1)	114.37	126.75	48.42
H-5(Z1CS1)	114.76	127.37	46.12
H-5(Z2CS1)	114.52	126.64	46.42

Table 6
Thermal parameters of composite samples (CNCs/B_2O_3) from TGA.

Formulation	T_{onset} (°C)	T_{50} (°C)	T_{endset} (°C)	Residue wt. (%)
Pure HDPE	457.80	480.97	497.91	0.0025
H-3CS	465.80	484.58	501.56	1.1701
H-5CS	466.16	484.95	499.92	2.6849
H-3(B1CS1)	467.25	483.31	502.27	3.7349
H-3(B2CS1)	466.71	483.12	501.55	3.6572
H-5(B1CS1)	468.26	485.13	504.90	3.8370
H-5(B2CS1)	465.43	488.48	505.29	3.8704

be the presence of oleic acid, which was incorporated into the boron oxide structure. The lower flash point of oleic acid (189.9 °C) likely hindered further improvement of the composites T_{onset} [6].

On the other hand, the incorporation of ZnO in higher percentages resulted in an increase in the thermal stability of the composites, shifting final decomposition temperature to a higher value. This is because of the shielding effect of ZnO particles, which prevented thermal decomposition and pyrolysis of the cellulose.

Table 7
Thermal parameters of composite samples (CNCs/ZnO) from TGA.

Formulation	T_{onset} (°C)	T_{50} (°C)	T_{endset} (°C)	Residue wt. (%)
Pure HDPE	457.80	480.97	497.91	0.0025
H-3CS	465.80	484.58	501.56	1.1701
H-5CS	466.16	484.95	499.92	2.6849
H-3(Z1CS1)	467.25	484.30	503.09	3.7822
H-3(Z2CS1)	467.44	484.68	512.84	4.0833
H-5(Z1CS1)	467.80	489.72	508.26	3.6212
H-5(Z2CS1)	470.36	488.71	507.37	3.8561

Overall, the incorporation of ZnO-coated and B_2O_3-coated silane functionalized CNCs into the polymer matrix resulted in higher thermal stability compared with pure HDPE. All formulations containing ZnO demonstrated higher thermal stability in comparison with other formulations containing B_2O_3 and the composites with only silane-treated CNCs. This suggests a synergistic interaction between ZnO and CNCs and a relatively stronger network between them in the composites' structure [29]. The weight residue for all formulations with B_2O_3 and ZnO was higher than that of pure HDPE and samples with only silane-treated CNCs. This suggests that incorporating metal oxides into the composites has the potential to improve thermal stability.

3.6. *Horizontal burn test*

To investigate flame spread rate, weight loss of the composites and the effect of fire retardants on the composites, the horizontal burn test was done. The results are presented in Fig. 6, Table 8, and Table 9.

According to the results, the addition of silane-treated CNCs into HDPE did not have any effect on the flame spread rate and the weight loss of composites. Incorporating B_2O_3 led to a significant reduction in flame spread rate and weight loss compared with pure HDPE and composites containing only silane-treated CNCs. This decrease in weight loss and flame spread rate is due to the development of a glassy protective layer, which is characteristic of boron-based compounds [27]. Higher ratios of B_2O_3 did not have any significant impact on weight loss and flame spread rate, which can be because of the increased filler agglomerations in the composites with higher filler percentages, as evidenced in SEM images.

A similar trend was observed for composites with ZnO. ZnO acted as a catalyst to promote char formation and prevent oxygen penetration, thereby reducing weight loss and flame spread rate [24,39]. Similar to

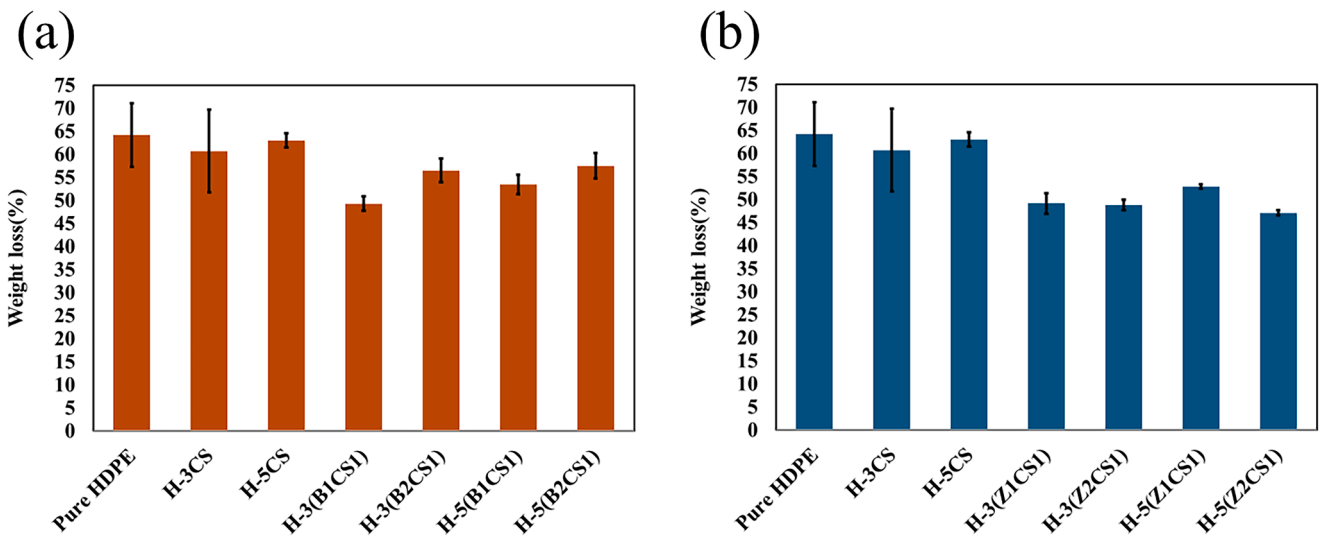

Fig. 6. Representative graphs of Weight loss (a) B_2O_3-coated CNCs composites and (b) ZnO-coated CNCs composites.

Table 8
Flame spread rate (mm/s) and Weight-Loss (%) values of different formulations containing B_2O_3.

Formulation	flame Spread Rate (mm/s)	Weight-Loss (%)
Pure HDPE	1.88 ± 0.10^{a}	64.15 ± 6.89^{a}
H-3CS	1.90 ± 0.57^{a}	$60.71\pm8.96^{a,b}$
H-5CS	1.93 ± 0.10^{a}	63.04 ± 1.55^{a}
H-3(B1CS1)	1.00 ± 0.12^{b}	49.30 ± 1.52^{c}
H-3(B2CS1)	0.91 ± 0.09^{b}	$56.51\pm2.56^{a,b,c}$
H-5(B1CS1)	1.13 ± 0.11^{b}	$53.46\pm2.08^{b,c}$
H-5(B2CS1)	1.05 ± 0.14^{b}	$57.70\pm2.74^{a,b}$

* Values (mean ± SD) in each column with different letters are significantly different from one another, according to Fisher's least significant difference test at $\alpha = 0.05$.

Table 9
Flame spread rate (mm/s) and Weight-Loss (%) values of different formulations containing ZnO.

Formulation	flame Spread Rate (mm/s)	Weight-Loss (%)
Pure HDPE	1.88 ± 0.10^{a}	64.15 ± 6.89
H-3CS	1.90 ± 0.57^{a}	60.71 ± 8.96^{a}
H-5CS	1.93 ± 0.10^{a}	63.00 ± 1.55^{a}
H-3(Z1CS1)	1.09 ± 0.09^{b}	49.13 ± 2.27^{b}
H-3(Z2CS1)	0.96 ± 0.05^{b}	48.57 ± 1.15^{b}
H-5(Z1CS1)	0.97 ± 0.18^{b}	52.78 ± 0.44^{b}
H-5(Z2CS1)	0.81 ± 0.03^{b}	47.10 ± 0.59^{b}

* Values (mean ± SD) in each column with different letters are significantly different from one another, according to Fisher's least significant difference test at $\alpha = 0.05$.

composite samples containing boron oxide, higher ratios of ZnO did not show any significant change in the results.

In general, the incorporation of inorganic metal oxides led to a notable decrease in both weight loss and flame spread rate in the composites. Overall, composites with boron oxide exhibited a 23 % decrease in weight loss, while those with zinc oxide showed a 28 % decrease.

3.7. Microcalorimetry test

The microscale combustion test was conducted to evaluate the heat release capacity (J/gK), peak heat release rate (W/g), and total heat release (kJ/g) of the composite samples. The results are shown in Fig. 7 and Table 10. The heat release rate (HRR) is determined by multiplying a material's mass loss rate with its heat of combustion [40]. It is a critical factor in managing fire risks, as HRR serves as the primary driving force behind the spread of fire. Total heat release (total HR) quantifies the overall energy released, which shows how much energy the material contributes to fire. The peak heat release rate (Pk-HRR) helps evaluate how intensely the material can burn. Temperature of peak heat release rate (T-pHRR) is the temperature at which material reaches its highest heat release rate during combustion. In the horizontal burn test, it was observed that the samples containing only silane-functionalized CNCs did not show any effect on flame spread rate and weight loss. As a result, four formulations, H-3(B2CS1), H-5(B2CS1), H-3(Z2CS1), and H-5 (Z2CS1) were picked to compare the fire-retardant properties of inorganic metal oxides.

In combustion, the breakdown of the resin matrix results in the emission of flammable volatiles, and the fire retardant (filler) plays a crucial role in limiting the heat released from the polymer composite. The initial delay phase, lasting until around 400 °C, occurred because the composite's temperature was not yet at the pyrolysis point of the HDPE matrix. During this period, heat release remained minimal, as the material had not started to decompose or produce volatile products for combustion. The heat release rate (HRR) experienced a sharp rise after the initial induction phase, marking the onset of volatile combustion at the composite-fire interface. At around 500 °C, the peak heat release rate (PHRR) was reached. After a brief stability, the heat output dropped significantly. The char layer formed on the surface of the exposed polymer acted as a barrier, reducing the escape of volatile gases, including low-molecular-weight hydrocarbons. This led to a slower decomposition of the underlying material. Additionally, the reduced resin content in the composites contributed to the lower PHRR. Both formulations containing B_2O_3 showed a slight improvement in fire resistance compared to pure HDPE. Heat release (HR) capacity, peak heat release rate (Pk-HRR) values were marginally reduced. Generally, the reduction in HRR can be attributed to the fact that the addition of boron oxide causes the formation of a glassy protective layer on the surface during combustion, which acts as a barrier, reducing the release of volatile compounds and preventing oxygen access [41].

ZnO-coated CNC composites with 3 % filler showed similar results to those with B_2O_3, with marginally lower values in HR capacity, Pk-RR, and total HR for this formulation. However, ZnO-coated composites with higher filler concentration did not show any difference compared with pure HDPE. The reason for this observation can be the particle agglomerations in higher filler concentrations [6]. Overall, while TGA and horizontal fire test results show more improvement in fire resistance properties of the composites, there is only a marginal difference in the

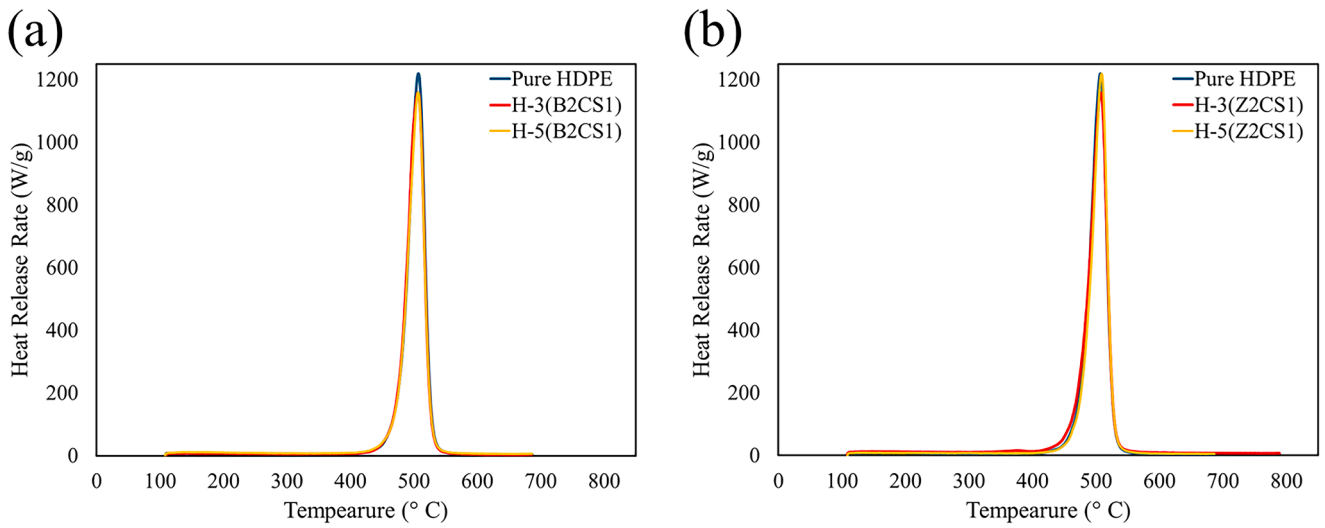

Fig. 7. Representative graphs of Heat Release rate (a) B_2O_3-coated CNCs composites and (b) ZnO-coated CNCs composites.

Table 10
Microcalorimetry test results of Pure HDPE and composite samples containing B_2O_3 and ZnO.

Formulation	HR capacity (J/g. K)	Pk—HRR (W/g)	Total HR (kJ/g)	T-pHRR
Pure HDPE	1241.0	1214.0	41.0	507.1
H-3(B2CS1)	1176.0	1151.0	40.0	506.8
H-5(B2CS1)	1180.0	1151.0	38.9	507.0
H-3(Z2CS1)	1169.0	1148.0	38.5	508.7
H-5(Z2CS1)	1235.0	1212.0	41.2	507.4

microcalorimetry test results for the composites in comparison with pure HDPE. The discrepancy in the results can be attributed to the fire retardancy mode mechanisms of nano ZnO and B_2O_3. The small change in heat release rate (HRR) for the composites containing ZnO and B_2O_3 suggests that ZnO and B_2O_3 primarily act in the condensed phase. Fire retardants that work in the condensed phase influence mass loss and char formation, and their incorporation may not significantly affect gas-phase combustion, resulting in minimal HRR reductions [42].

4. Conclusion

This study investigated the effect of incorporating nano boron oxide and nano zinc oxide coated silane-treated cellulose nanocrystals into high-density polyethylene to enhance its mechanical, thermal, and flame-retardant properties. The results demonstrated that these inorganic metal oxide fillers improve the composites' mechanical strength, thermal stability, and fire resistance significantly. The incorporation of ZnO- and B_2O_3-coated CNCs significantly improved the storage modulus of the composites, with 64 % and 52 % increase for ZnO and B_2O_3-coated CNCs, respectively, compared to pure HDPE. The improvement in the mechanical properties of the composites was attributed to the strong interfacial bonding between the fillers and the polymer matrix, leading to reduced polymer chain mobility and higher stiffness. Thermogravimetric analysis (TGA) showed that the addition of ZnO led to a shift in decomposition temperature, indicating improved resistance to thermal degradation. Similarly, B_2O_3 increased residue formation, which is an indicative of enhanced char formation. The horizontal burn test revealed a decrease in flame spread rate and weight loss of the composites containing nano ZnO and B_2O_3. The composites with nano B_2O_3 and ZnO exhibited a 23 % and 28 % reduction in weight loss, respectively, suggesting their effectiveness in improving flame retardancy. However, despite these improvements in thermal and burn resistance, the microcalorimetry test showed only a marginal reduction in heat release rate (HRR). This discrepancy is likely due to the primary condensed-phase action of ZnO and B_2O_3, which enhances char formation rather than actively inhibiting gas-phase radical reactions. The insights from this research are particularly relevant for industries such as automotive, construction, and packaging, where fire resistance and mechanical durability are critical. The use of bio-based CNCs and environmentally friendly metal oxides aligns with the growing demand for sustainable polymer composites. These hybrid fillers offer a safer, eco-friendly alternative to traditional halogen-based flame retardants, reducing the environmental impact of petroleum-based materials. Compared to conventional flame retardants, such as halogenated compounds or phosphorus-based additives, the incorporation of ZnO and B_2O_3-coated CNCs into HDPE composites offers several advantages in terms of efficiency, cost, and environmental impact. Traditional flame retardants often require higher loading levels to achieve significant fire resistance. In contrast, metal oxide fillers have shown comparable or superior flame retardancy at much lower concentrations. The cost of CNCs is relatively low due to their abundant availability from biomass sources. While metal oxides like ZnO and B_2O_3 may have higher initial costs than some traditional additives, their effectiveness at lower loadings reduces overall material usage.

Disclaimer

Mention of trade names or commercial products in this publication is solely for the purpose of providing specific information and does not imply recommendation or endorsement by the U.S. Department of Agriculture. USDA is an equal opportunity provider and employer.

CRediT authorship contribution statement

Amirmohammad Raeisi: Writing – original draft, Visualization, Methodology, Investigation, Formal analysis, Data curation. **Ismat Ara:** Writing – review & editing, Visualization, Validation. **Greg Holt:** Writing – review & editing, Visualization, Resources. **Nicole Stark:** Conceptualization, Funding acquisition, Resources. **Dilpreet S. Bajwa:** Writing – review & editing, Supervision, Resources, Project administration, Funding acquisition, Conceptualization.

Declaration of competing interest

The authors declare that they have no known competing financial interests or personal relationships that could have appeared to influence

the work reported in this paper.

Acknowledgement

The research was funded by U.S. National Institute of Standards and Technology (NIST), grant number 70NANB18H256N.

References

[1] J. Jo, H. Kim, S.-Y. Jeong, C. Park, H.S. Hwang, B. Koo, Changes in mechanical properties of polyhydroxyalkanoate with double silanized cellulose nanocrystals using different organosiloxanes, Nanomaterials 11 (6) (2021) 1542, https://doi.org/10.3390/nano11061542.

[2] T. Aziz, A. Ullah, A. Ali, M. Shabeer, M.N. Shah, F. Haq, M. Iqbal, R. Ullah, F. U. Khan, Manufactures of bio-degradable and bio-based polymers for bio-materials in the pharmaceutical field, J. Appl. Polym. Sci. 139 (29) (2022), https://doi.org/10.1002/app.52624.

[3] L. Liu, M. Zhu, J. Feng, H. Peng, Y. Shi, J. Gao, L. Tang, P. Song, Fire-retardant and high-strength polymeric materials enabled by supramolecular aggregates, Aggregate 5 (2) (2024), https://doi.org/10.1002/agt2.494.

[4] D.C. CRACIUN, I. PETER, Review of the polymeric material composite, optimization for industrial application, Acta Marisiensis. Seria Technologica 21 (1) (2024) 47–51, https://doi.org/10.62838/amset-2024-0008.

[5] K. Matsumoto, T. Tanaka, M. Sasada, N. Sano, K. Masuyama, A mechanism for fire retardancy realized by a combination of biofillers and ammonium polyphosphate in various polymer systems, Cellulose 28 (6) (2021) 3833–3846, https://doi.org/10.1007/s10570-021-03747-4.

[6] D.S. Bajwa, G. Holt, N. Stark, S.G. Bajwa, S. Chanda, M. Quadir, Nano boron oxide and zinc oxide doped lignin containing cellulose nanocrystals improve the thermal, mechanical and flammability properties of high-density poly(Ethylene), Polymers. (Basel) 16 (1) (2023) 36, https://doi.org/10.3390/polym16010036.

[7] Y. Huang, S. Jiang, R. Liang, Z. Liao, G. You, A green highly-effective surface flame-retardant strategy for rigid polyurethane foam: transforming UV-cured coating into intumescent self-extinguishing layer, Compos. Part a Appl. Sci. Manuf. 125 (2019) 105534, https://doi.org/10.1016/j.compositesa.2019.105534.

[8] W. Zhang, Y. Lei, X. Li, H. Shao, W. Xu, D.A Facile Li, Environmentally and friendly flame-retardant: synergistic flame retardant property of polyurethane rigid foam, Mater. Lett. 267 (2020) 127542, https://doi.org/10.1016/j.matlet.2020.127542.

[9] H. Peng, X. Wang, T. Li, C. Lou, Y. Wang, J. Lin, Mechanical properties, thermal stability, sound absorption, and flame retardancy of rigid PU foam composites containing a fire-retarding agent: effect of magnesium hydroxide and aluminum hydroxide, Polym. Adv. Technol. 30 (8) (2019) 2045–2055, https://doi.org/10.1002/pat.4637.

[10] L. Qian, L. Li, Y. Chen, B. Xu, Y. Qiu, Quickly self-extinguishing flame retardant behavior of rigid polyurethane foams linked with phosphaphenanthrene groups, Compos. B Eng. 175 (2019) 107186, https://doi.org/10.1016/j.compositesb.2019.107186.

[11] C. Wang, Y. Wu, Y. Li, Q. Shao, X. Yan, C. Han, Z. Wang, Z. Liu, Z. Guo, Flame-retardant rigid polyurethane foam with a phosphorus-nitrogen single intumescent Flame retardant, Polym. Adv. Technol. 29 (1) (2018) 668–676, https://doi.org/10.1002/pat.4105.

[12] J. Wu, X. Zhang, Z. Qin, W. Zhang, R. Yang, Inorganic/organic phosphorus-based flame retardants synergistic flame retardant rigid polyurethane foam, Polym. Eng. Sci. 63 (3) (2023) 1041–1049, https://doi.org/10.1002/pen.26264.

[13] C.C. Carignan, W. Heiger-Bernays, M.D. McClean, S.C. Roberts, H.M. Stapleton, A. Sjödin, T.F. Webster, Flame retardant exposure among collegiate United States gymnasts, Environ. Sci. Technol. 47 (23) (2013) 13848–13856, https://doi.org/10.1021/es4037868.

[14] I. van der Veen, J. de Boer, Phosphorus flame retardants: properties, production, environmental occurrence, toxicity and analysis, Chemosphere 88 (10) (2012) 1119–1153, https://doi.org/10.1016/j.chemosphere.2012.03.067.

[15] T. Aziz, A. Farid, F. Haq, M. Kiran, A. Ullah, K. Zhang, C. Li, S. Ghazanfar, H. Sun, R. Ullah, A. Ali, M. Muzammal, M. Shah, N. Akhtar, S. Selim, N. Hagagy, M. Samy, S.K. Al Jaouni, A review on the modification of cellulose and its applications, Polymers. (Basel) 14 (15) (2022) 3206, https://doi.org/10.3390/polym14153206.

[16] J. Shojaeiarani, D. Bajwa, G. Holt, Sonication amplitude and processing time influence the cellulose nanocrystals morphology and dispersion, Nanocomposites 6 (1) (2020) 41–46, https://doi.org/10.1080/20550324.2019.1710974.

[17] D.S. Bajwa, C. Rehovsky, J. Shojaeiarani, N. Stark, S. Bajwa, M.A. Dietenberger, Functionalized cellulose nanocrystals: a potential fire retardant for polymer composites, Polymers. (Basel) 11 (8) (2019) 1361, https://doi.org/10.3390/polym11081361.

[18] P.T. Williams, P.A. Horne, The role of metal salts in the pyrolysis of biomass, Renew. Energy 4 (1) (1994) 1–13, https://doi.org/10.1016/0960-1481(94)90058-2.

[19] H.R. Favarim, L.O. Leite, Performance of ZnO nanoparticles for fire retardant and UV protection of pine wood, Bioresources 13 (3) (2018) 6963–6969, https://doi.org/10.15376/biores.13.3.6963-6969.

[20] T. Aziz, W. Li, J. Zhu, B. Chen, Developing multifunctional cellulose derivatives for environmental and biomedical applications: insights into modification processes and advanced material properties, Int. J. Biol. Macromol. 278 (2024) 134695, https://doi.org/10.1016/j.ijbiomac.2024.134695.

[21] S. Chanda, D.S. Bajwa, G.A. Holt, N. Stark, S.G. Bajwa, M. Quadir, Silane compatibilzation to improve the dispersion, thermal and mechancial properties of cellulose nanocrystals in poly (Ethylene Oxide), Nanocomposites 7 (1) (2021) 87–96, https://doi.org/10.1080/20550324.2021.1942641.

[22] S. Saleemi, H.A. Mannan, T. Riaz, A.M. Hai, H. Zeb, A.K. Khan, Optimizing synergistic silica–Zinc oxide coating for enhanced flammability resistance in cotton protective clothing, Fibers 12 (5) (2024) 44, https://doi.org/10.3390/fib12050044.

[23] K. Bansal, S. Mansouri, D. Bajwa, S. Swarup, M. Quadir, Synthesis of phytic acid-layered zinc oxide hybrid nanoparticles and their flame-retardant applications in polyurethane coatings, J. Coat. Technol. Res. 21 (1) (2024) 369–382, https://doi.org/10.1007/s11998-023-00828-w.

[24] Y.-W. Wang, R. Shen, Q. Wang, Y. Vasquez, ZnO microstructures as flame-retardant coatings on cotton fabrics, ACS. Omega 3 (6) (2018) 6330–6338, https://doi.org/10.1021/acsomega.8b00371.

[25] M. Dogan, S.D. Dogan, L.A. Savas, G. Ozcelik, U. Tayfun, Flame retardant effect of boron compounds in polymeric materials, Compos. B Eng. 222 (2021) 109088, https://doi.org/10.1016/j.compositesb.2021.109088.

[26] S. Tang, L. Qian, X. Liu, Y. Dong, Gas-phase flame-retardant effects of a Bi-group compound based on phosphaphenanthrene and triazine-trione groups in epoxy resin, Polym. Degrad. Stab. 133 (2016) 350–357, https://doi.org/10.1016/j.polymdegradstab.2016.09.014.

[27] O. Polat, C. Kaynak, Use of boron oxide and boric acid to improve flame retardancy of an organophosphorus compound in neat and Fiber reinforced polyamide-6, J Vinyl Addit Technol 22 (3) (2016) 300–310, https://doi.org/10.1002/vnl.21445.

[28] P. Xu, Y. Cao, B. Wu, P. Ma, W. Dong, H. Bai, H. Zhang, H. Zhu, M. Chen, Effects of modified nanocrystalline cellulose on the hydrophilicity, crystallization and mechanical behaviors of poly(3-Hydroxybutyrate- *Co* -3-Hydroxyhexanoate), New. J. Chem. 42 (14) (2018) 11972–11978, https://doi.org/10.1039/C8NJ02012D.

[29] D.S. Bajwa, J. Shojaeiarani, J.D. Liaw, S.G. Bajwa, Role of hybrid nano-zinc oxide and cellulose nanocrystals on the mechanical, thermal, and flammability properties of poly (Lactic Acid) polymer, J. Compos. Sci. 5 (2) (2021) 43, https://doi.org/10.3390/jcs5020043.

[30] J. Shojaeiarani, D.S. Bajwa, N.M. Stark, S.G. Bajwa, Rheological properties of cellulose nanocrystals engineered polylactic acid nanocomposites, Compos. B Eng. 161 (2019) 483–489, https://doi.org/10.1016/j.compositesb.2018.12.128.

[31] J. Shojaeiarani, D.S. Bajwa, K. Hartman, Esterified cellulose nanocrystals as reinforcement in poly(Lactic Acid) nanocomposites, Cellulose 26 (4) (2019) 2349–2362, https://doi.org/10.1007/s10570-018-02237-4.

[32] J. Shojaeiarani, D.S. Bajwa, N.M. Stark, Spin-coating: a new approach for improving dispersion of cellulose nanocrystals and mechanical properties of poly (Lactic Acid) composites, Carbohydr. Polym. 190 (2018) 139–147, https://doi.org/10.1016/j.carbpol.2018.02.069.

[33] M.B. Salon, G. Gerbaud, M. Abdelmouleh, C. Bruzzese, S. Boufi, M.N. Belgacem, Studies of interactions between silane coupling agents and cellulose fibers with liquid and solid-state NMR, Magn. Reson. Chem. 45 (6) (2007) 473–483, https://doi.org/10.1002/mrc.1994.

[34] Chanda, Saptaparni. “Application of functionalized cellulose nanocrystals to improve their dispersion in polymer matrix and enhance the thermo-mechanical properties of polymer composites.” (2023).

[35] K. Karunakaran, S.S. Singh, R. Kitey, Investigating the role of filler shape on the dynamic mechanical properties of glass-filled epoxy composites, Polym. Compos. 43 (10) (2022) 6912–6925, https://doi.org/10.1002/pc.26737.

[36] O.A. Afolabi, N. Ndou, Synergy of hybrid fillers for emerging composite and nanocomposite materials—A review, Polymers. (Basel) 16 (13) (2024) 1907, https://doi.org/10.3390/polym16131907.

[37] X. Xu, F. Liu, L. Jiang, J.Y. Zhu, D. Haagenson, D.P. Wiesenborn, Cellulose nanocrystals vs. Cellulose nanofibrils: a comparative study on their microstructures and effects as polymer reinforcing agents, ACS. Appl. Mater. Interfaces. 5 (8) (2013) 2999–3009, https://doi.org/10.1021/am302624t.

[38] N. Bitinis, R. Verdejo, J. Bras, E. Fortunati, J.M. Kenny, L. Torre, M.A. López-Manchado, Poly(Lactic Acid)/natural rubber/cellulose nanocrystal bionanocomposites part I. Processing and morphology, Carbohydr. Polym. 96 (2) (2013) 611–620, https://doi.org/10.1016/j.carbpol.2013.02.068.

[39] J. Shojaeiarani, D. Bajwa, L. Jiang, J. Liaw, K. Hartman, Insight on the influence of nano zinc oxide on the thermal, dynamic mechanical, and flow characteristics of poly(Lactic Acid)– Zinc oxide composites, Polym. Eng. Sci. 59 (6) (2019) 1242–1249, https://doi.org/10.1002/pen.25107.

[40] J. Alongi, G. Malucelli, Cotton flame retardancy: state of the art and future perspectives, RSC. Adv. 5 (31) (2015) 24239–24263, https://doi.org/10.1039/C5RA01176K.

[41] G.-F. Wu, M. Xu, Effects of boron compounds on the mechanical and fire properties of wood-chitosan and high-density polyethylene composites, Bioresources 9 (3) (2014), https://doi.org/10.15376/biores.9.3.4173-4193.

[42] B. Schartel, T.R. Hull, Development of fire-retarded materials—Interpretation of cone calorimeter data, Fire Mater. 31 (5) (2007) 327–354, https://doi.org/10.1002/fam.949.